Topological Effects

PH671 - Transport

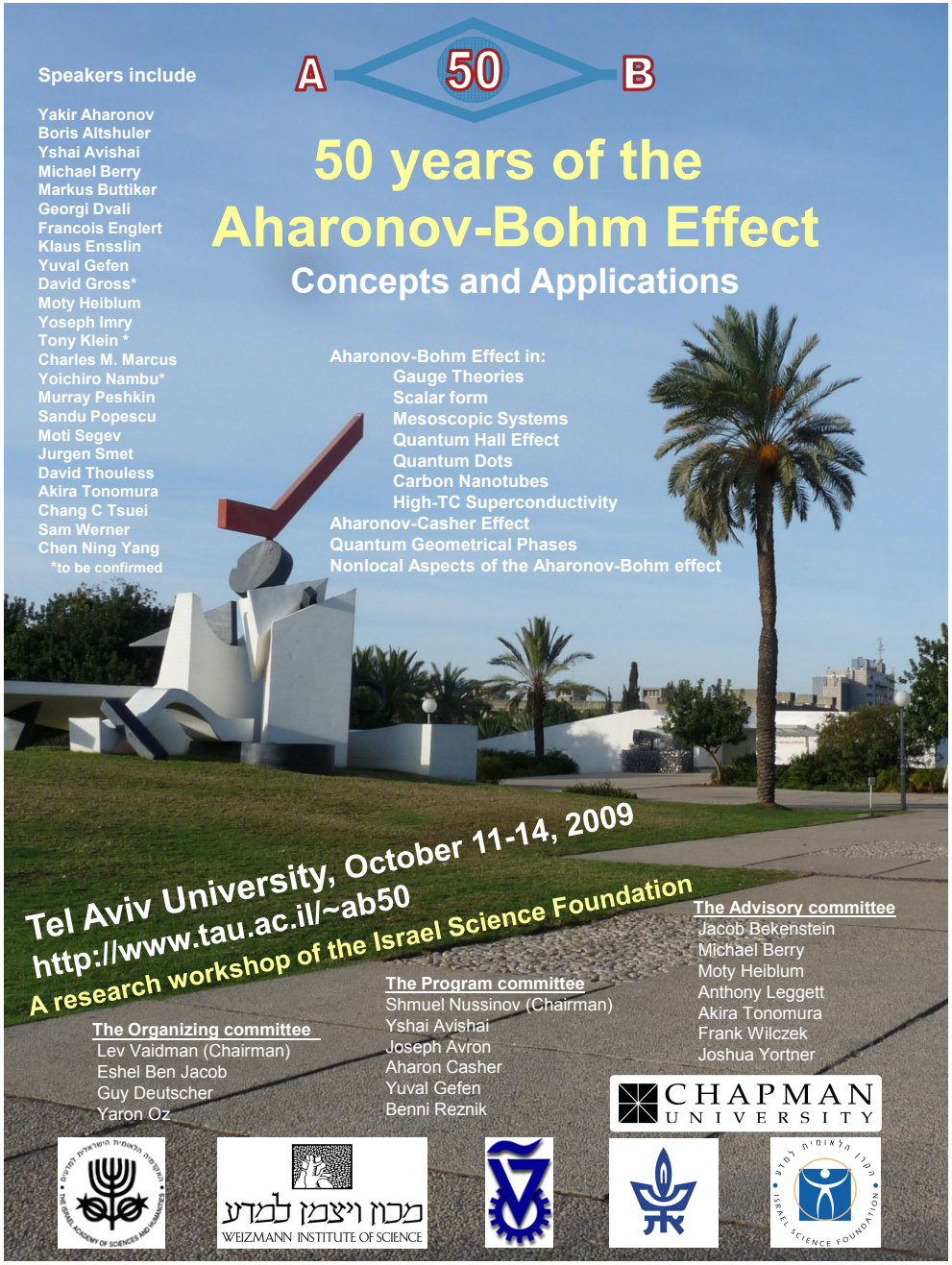
A 50 B
Speakers include
Yakir Aharonov
Boris Altshuler
Yshai Avishai
Michael Berry
Markus Buttiker
Georgi Dvali
Francois Englert
Klaus Ensslin
Yuval Gefen
David Gross*
Moty Heiblum
Yoseph Imry
Tony Klein *
Charles M. Marcus
Yoichiro Nambu*
Murray Peshkin
Sandu Popescu
Moti Segev
Jurgen Smet
David Thouless
Akira Tonomura
Chang C Tsuei
Sam Werner
Chen Ning Yang
*to be confirmed
50 years of the
Aharonov-Bohm Effect
Concepts and Applications
Aharonov-Bohm Effect in:
Gauge Theories
Scalar form
Mesoscopic Systems
Quantum Hall Effect
Quantum Dots
Carbon Nanotubes
High-TC Superconductivity
Aharonov-Casher Effect
Quantum Geometrical Phases
Nonlocal Aspects of the Aharonov-Bohm effect
Tel Aviv University, October 11-14, 2009
http://www.tau.ac.il/~ab50
A research workshop of the Israel Science Foundation
The Organizing committee
Lev Vaidman (Chairman)
Eshel Ben Jacob
Guy Deutscher
Yaron Oz
The Program committee
Shmuel Nussinov (Chairman)
Yshai Avishai
Joseph Avron
Aharon Casher
Yuval Gefen
Benni Reznik
The Advisory committee
Jacob Bekenstein
Michael Berry
Moty Heiblum
Anthony Leggett
Akira Tonomura
Frank Wilczek
Joshua Yortner
CHAPMAN UNIVERSITY
WEIZMANN INSTITUTE OF SCIENCE
ISRAEL SCIENCE FOUNDATION

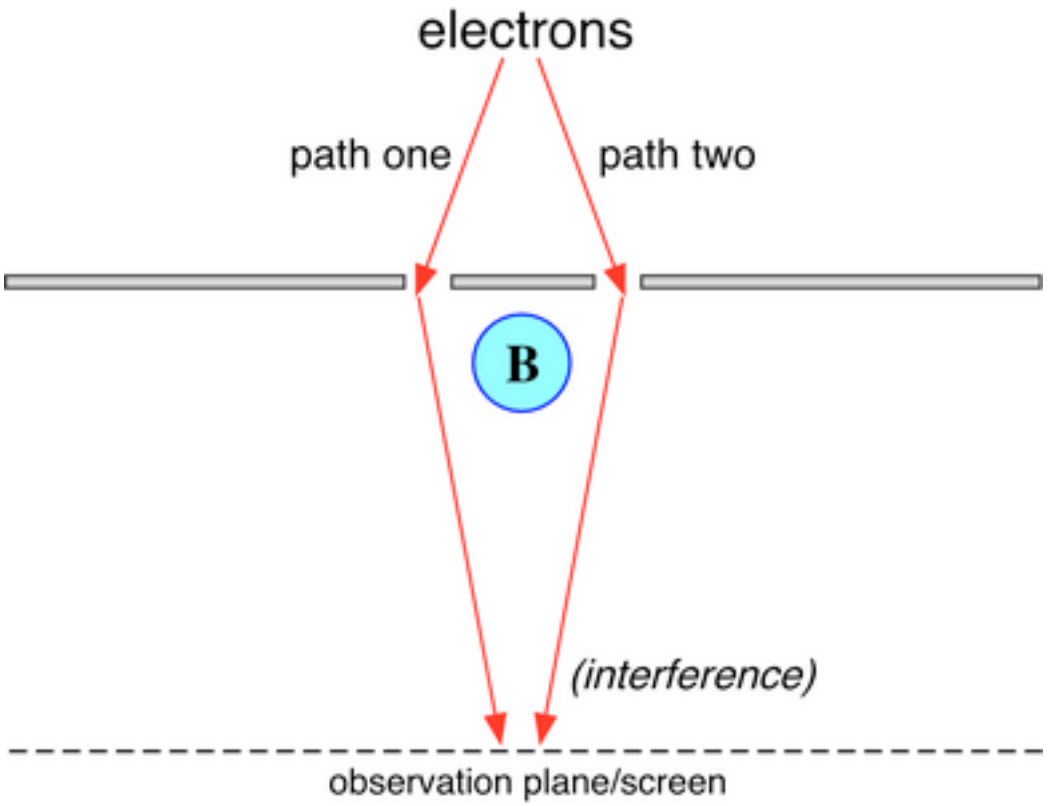
electrons
path one
path two
B
(interference)
observation plane/screen

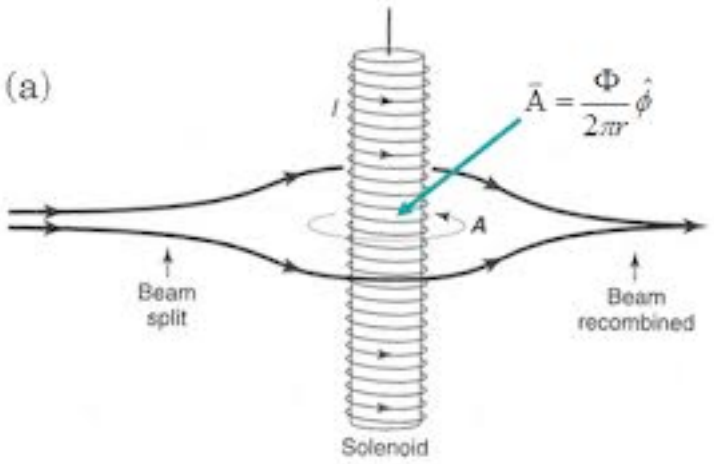
(a)
I
$\bar{A} = \frac{\Phi}{2\pi r}\hat{\phi}$
A
Beam split
Beam recombined
Solenoid

Observation of *h*/*e* Aharonov-Bohm Oscillations in Normal-Metal Rings
R. A. Webb, S. Washburn, C. P. Umbach, and R. B. Laibowitz
Phys. Rev. Lett. 54, 2696 – Published 24 June 1985

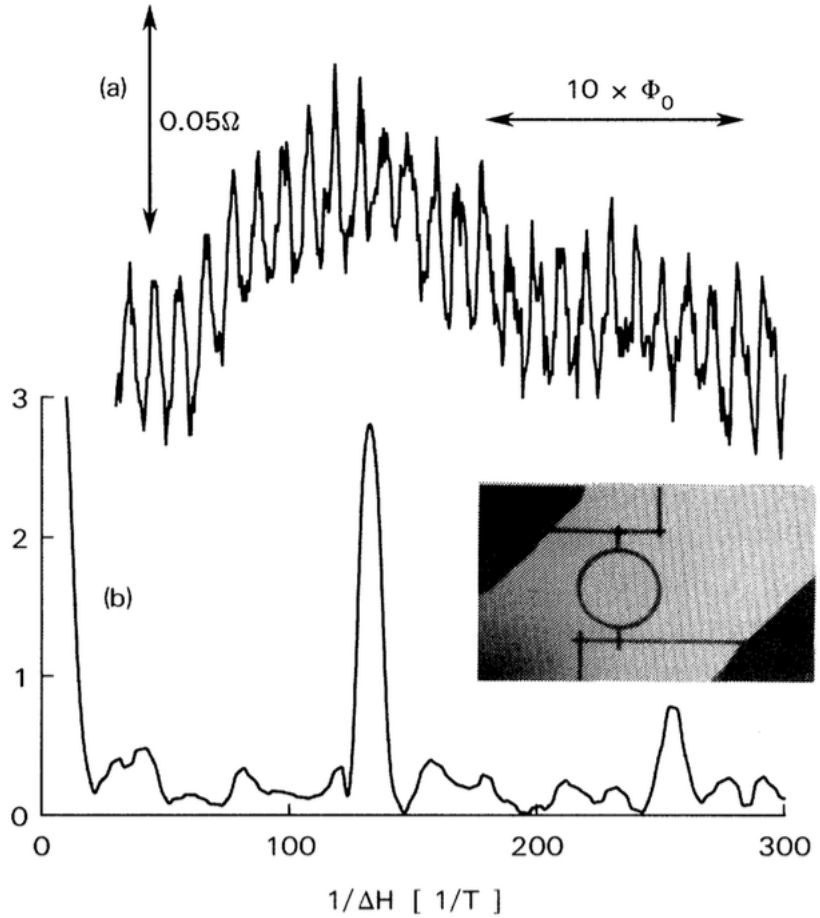

FIG. 1. (a) Magnetoresistance of the ring measured at $T = 0.01$ K. (b) Fourier power spectrum in arbitrary units containing peaks at h/e and $h/2e$. The inset is a photograph of the larger ring. The inside diameter of the loop is 784 nm, and the width of the wires is 41 nm.

Electromagnetic Aharonov-Bohm effect in a two-dimensional electron gas ring

W. G. van der Wiel, Yu. V. Nazarov, S. De Franceschi, T. Fujisawa, J. M. Elzerman, E. W. G. M. Huizeling, S. Tarucha, and L. P. Kouwenhoven

Phys. Rev. B 67, 033307 – Published 29 January 2003

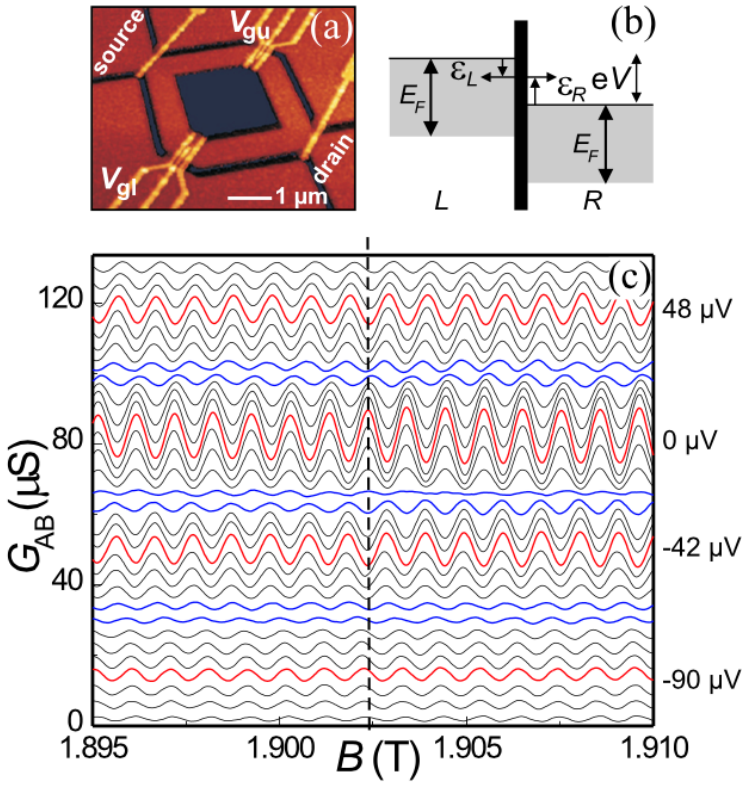

FIG. 1. (a) Atomic force microscope image of the device. The AB ring is defined in a 2DEG by dry etching (dark regions, depth $\sim$ 75 nm). The 2DEG with electron density $3.4 \times 10^{15} m^{-2}$ is situated 100 nm below the surface of an AlGaAs/GaAs heterostructure. In both arms of the ring (lithographic width 0.5 μm; perimeter 6.6 μm) a barrier can be defined by applying negative voltages to the gate electrodes V_{gu} and V_{gl}. The other gates are not used. (b)Schematic energy picture at one of the barriers (see text). (c) Differential AB conductance, G_{AB}, as function of B at 15 mK for different source drain voltages, V, separated by 5.3μV. The traces have a vertical offset. Three values for V are indicated on the right. The dashed line highlights a phase change by a change in the amplitude and sign of the AB oscillations, indicating an electrostatic AB effect.

Aharonov-Bohm effect in charge-density wave loops with inherent temporal current switching

M. Tsubota, K. Inagaki, T. Matsuura and S. Tanda

EPL, 97 (2012) 57011
doi: 10.1209/0295-5075/97/57011

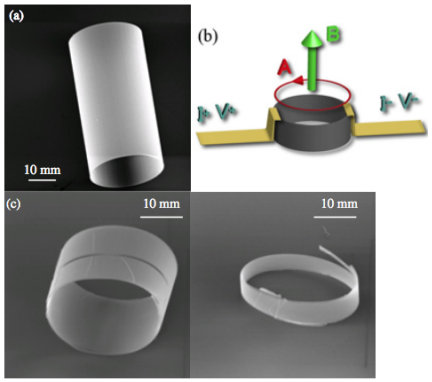

Fig. 1: (Colour on-line) (a) Scanning electron microscope (SEM) image of a TaS_3 tube-shaped crystal. (b) Contact configuration for transport measurement. Two gold electrodes (100 nm thick, 5 μm wide) were evaporated. (c) SEM image of a TaS_3 tube/ring crystal before cutting, (left) after cutting (right).

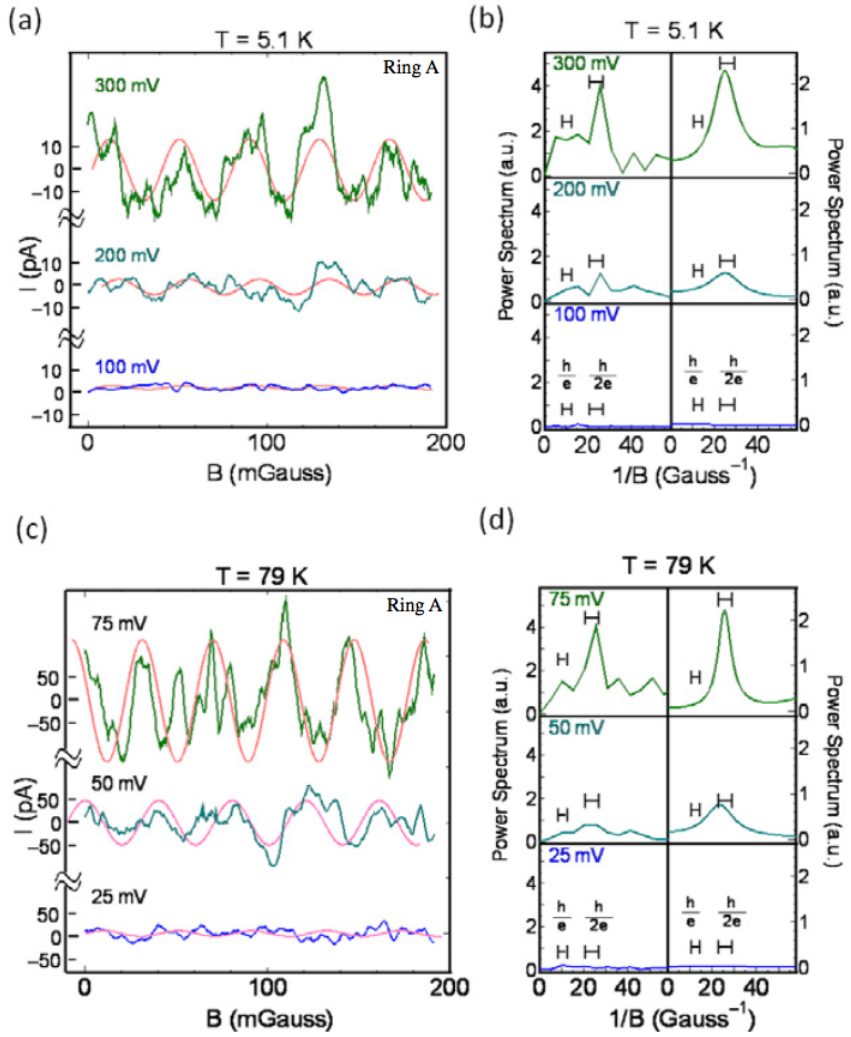

Fig. 2: (Colour on-line) (a) Change in current value as magnetic field at 5.1 K, applied voltage 100, 200 and 300 mV. (b) The power spectra of the observed oscillation using DFT (left) and MEM (right). The red lines show the sinusoidal oscillation estimated by IDFT and MEM. (c) Current depending on the magnetic field and (d) the evolution of the power spectra DFT (left) and MEM (right), 25, 50 and 75 mV, from bottom to top at 79 K.

Aharonov-Bohm effect in charge-density wave loops with inherent temporal current switching

M. Tsubota, K. Inagaki, T. Matsuura and S. Tanda

EPL, 97 (2012) 57011
doi: 10.1209/0295-5075/97/57011

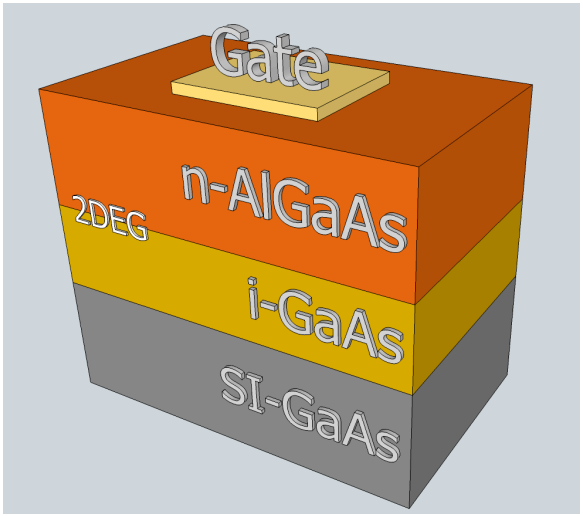

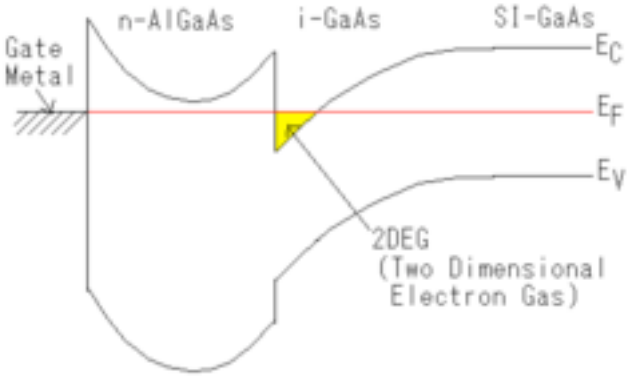

Interferometer-Based Studies of Quantum Hall Phenomena, Douglas T. McClure III (PhD thesis, Harvard, 2012)

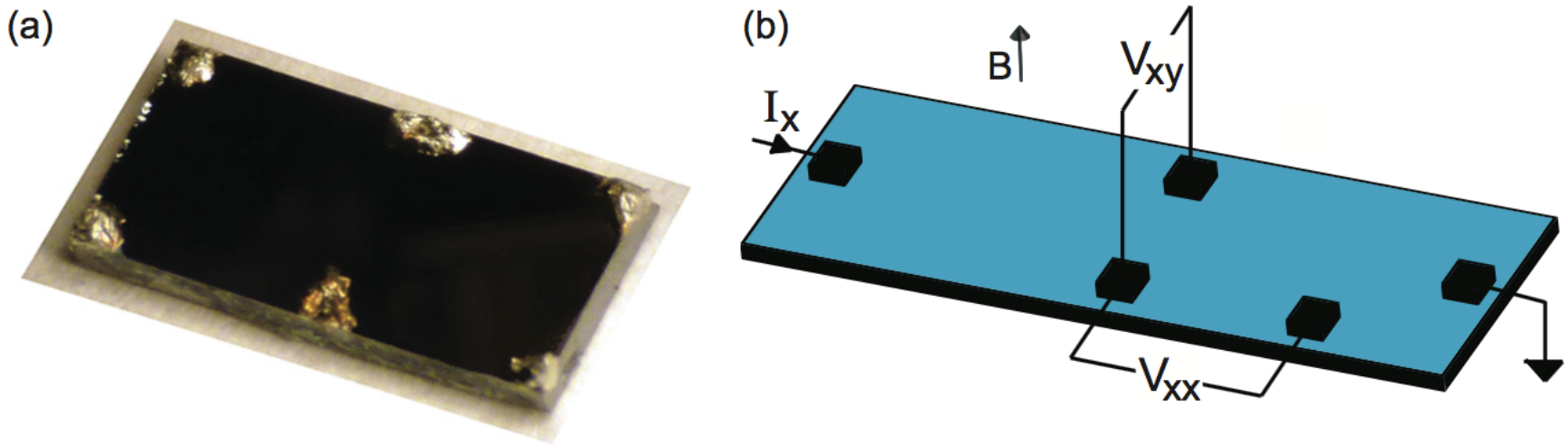

Figure 1.1: (a) GaAs Hall bar with six indium contacts. (b) Schematic Hall bar indicating a typical measurement configuration. A current bias I_x applied at one end of the sample gives rise to voltages V_{xy} and V_{xx}, from which the Hall and longitudinal resistances are calculated as $R_{xy} = V_{xy}/I_x$ and $R_{xx} = V_{xx}/I_x$.

Interferometer-Based Studies of Quantum Hall Phenomena, Douglas T. McClure III (PhD thesis, Harvard, 2012)

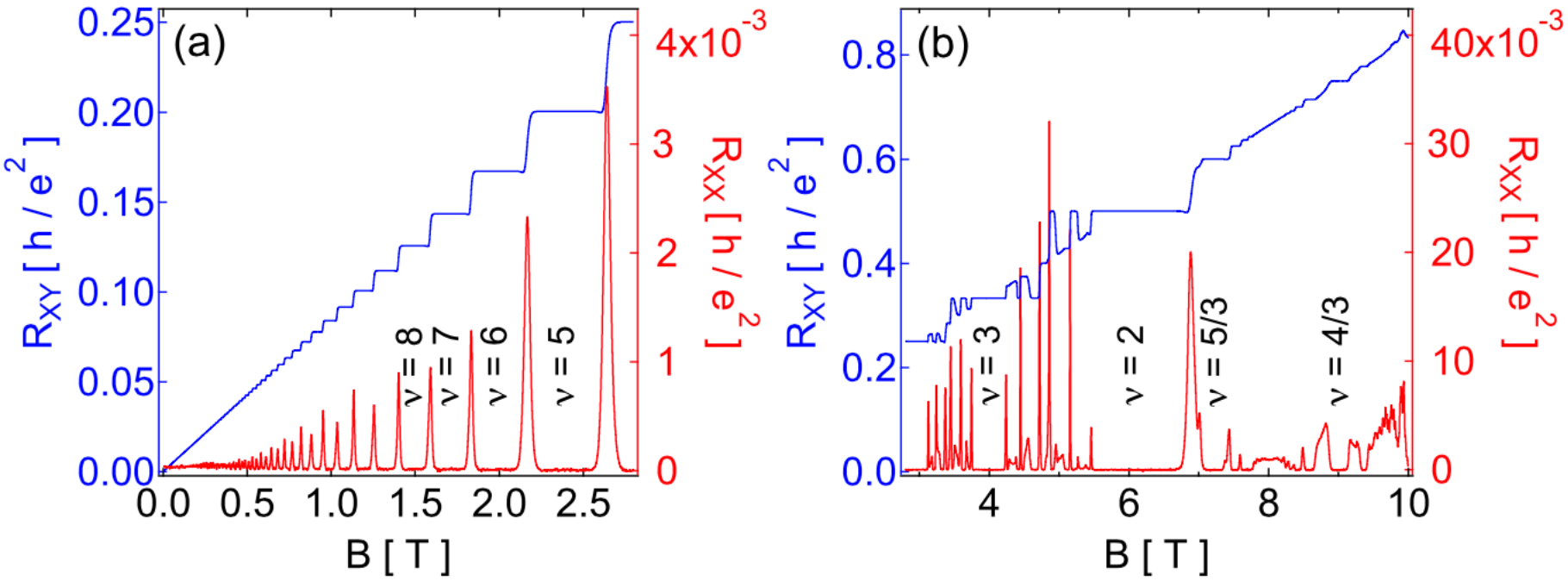

Figure 1.2: Hall (blue) and longitudinal (red) resistances as a function of magnetic field at a temperature of about 0.01 K. (a) As magnetic field is increased, a transition from classical to quantum Hall behavior is observed. (b) At even higher magnetic fields, the Hall resistance exhibits plateaus at fractional filling factors and even non-monotonic features.

The Composite Fermion: A Quantum Particle and Its Quantum Fluids

Jainendra K. Jain

Citation: Physics Today **53**(4), 39 (2000); doi: 10.1063/1.883035

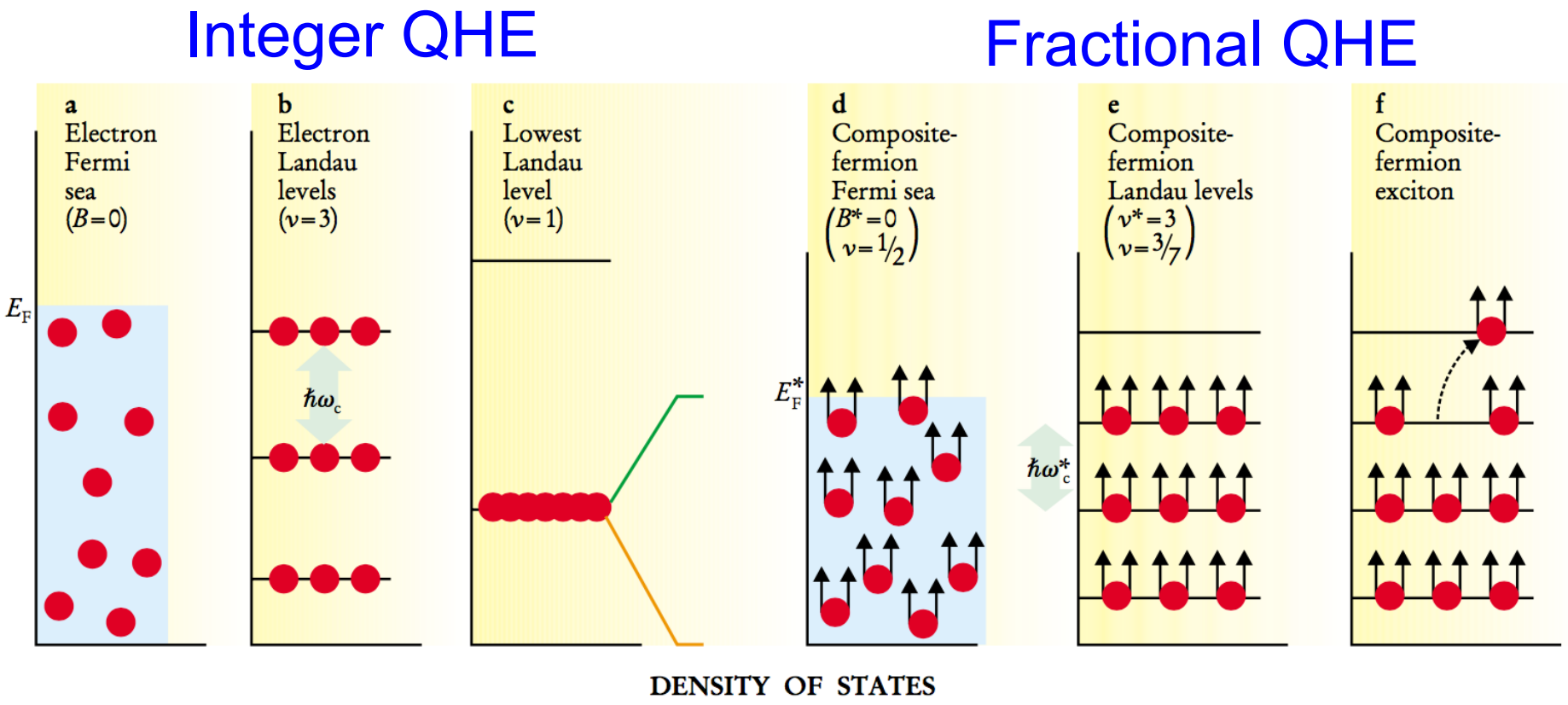

FIGURE 1. EVOLUTION OF A TWO-DIMENSIONAL ELECTRON SYSTEM as the transverse magnetic field B is increased. For independent electrons, the Fermi sea (**a**) (filled to Fermi energy E_F) at $B = 0$, splits into Landau levels (**b**) separated by the cyclotron energy. The lowest Landau level (**c**) is split by interactions into energy levels of composite fermions with attached flux quanta, which fill a composite-fermion Fermi sea (**d**) at $\nu = 1/2$ and occupy composite-fermion Landau levels (**e**) at other filling factors. A jump out of such a level (**f**) creates an exciton, a neutral particle–hole excitation. At still higher fields, this scenario (**d—f**) repeats itself, but now with composite fermions carrying four or more flux quanta.

The Composite Fermion: A Quantum Particle and Its Quantum Fluids

Jainendra K. Jain

Citation: Physics Today **53**(4), 39 (2000); doi: 10.1063/1.883035

Integer QHE

Fractional QHE

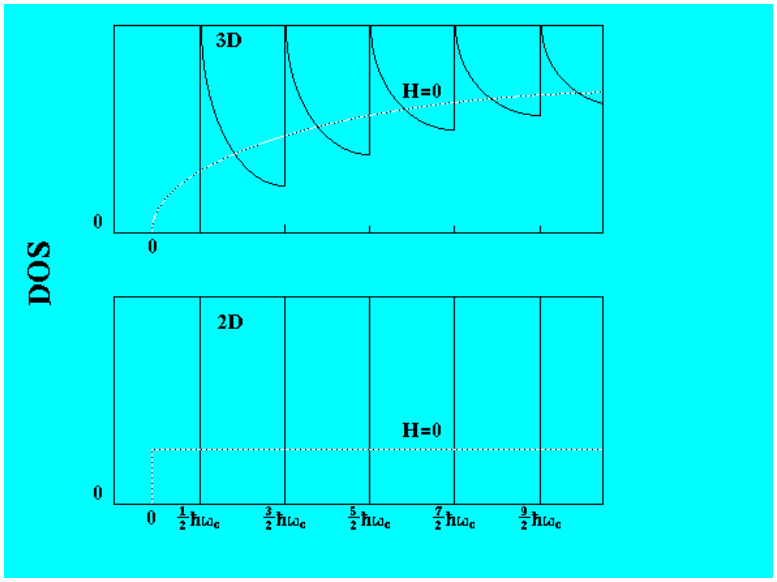

Interferometer-Based Studies of Quantum Hall Phenomena, Douglas T. McClure III (PhD thesis, Harvard, 2012)

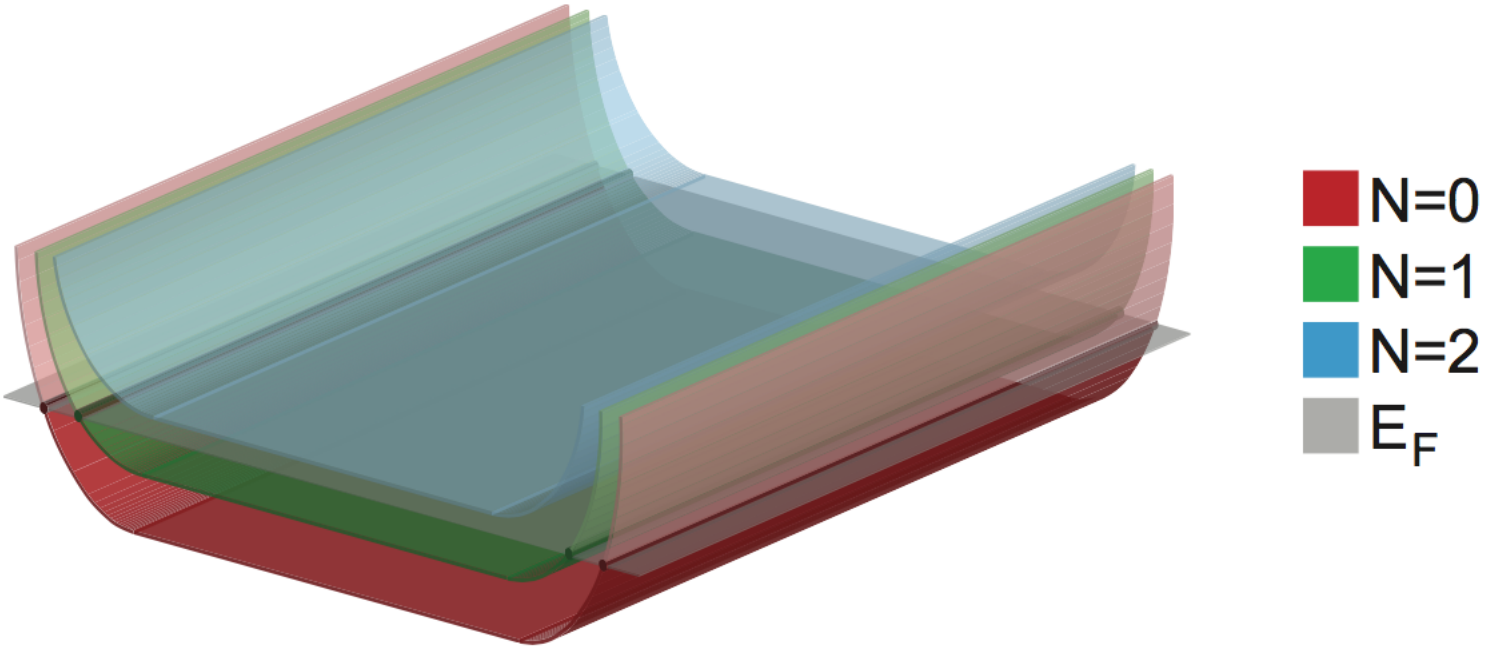

Figure 1.4: Schematic diagram of Landau levels in a 2DEG. In the bulk of the 2DEG, LL's below the Fermi energy are occupied. At the 2DEG edges, LL energies are bent upward by the confining potential, leading to the formation of chiral, current-carrying edge states.

Interferometer-Based Studies of Quantum Hall Phenomena, Douglas T. McClure III (PhD thesis , Harvard, 2012)
Chapter 2: Distinct signatures for Coulomb blockade and Aharonov-Bohm interference in electronic Fabry-Perot interferometers

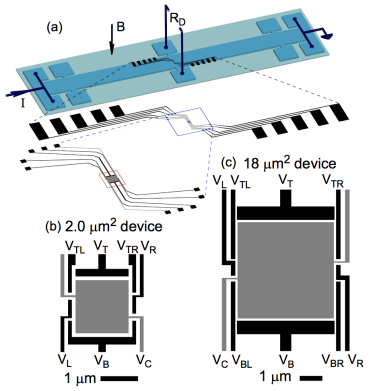

Figure 2.1: Measurement setup and devices. (a) Diagram of the wet-etched Hall bar, surface gates, and measurement configuration. Diagonal resistance, R_D, is measured directly across the Hall bar, with current bias, I. Subsequent zoom-ins of the surface gates are also shown; the red box encloses the detailed gate layouts for the device shown in (c). (b,c) Gate layouts for the 2.0 μm^2 and 18 μm^2 devices, respectively. The areas quoted refer to those under V_C.

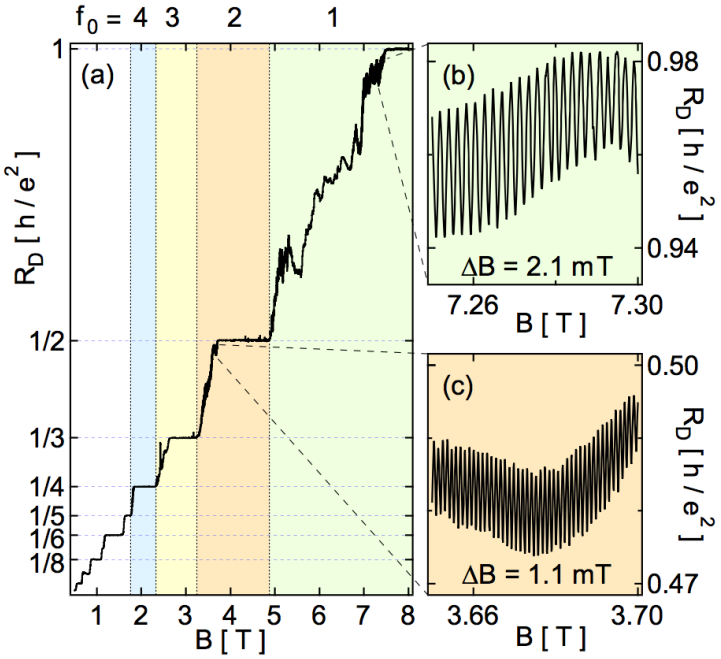

Figure 2.2: Oscillations in R_D as a function of magnetic field, B, for the 2.0 μm^2 device. (a) R_D as a function of B, showing well-quantized integer plateaus. Different colored backgrounds indicate different numbers of fully-occupied LL's, f_0, through the device. (b, c) Zoom-ins of the data in (a), at $f_0 = 1$ and 2, respectively, showing oscillations in R_D, and their B periods, ΔB.

[Experimental observation of the quantum Hall effect and Berry's phase in graphene]

Yuanbo Zhang, Yan-Wen Tan, Horst L. Stormer and Philip Kim

Nature 438, 201-204 (10 November 2005)
doi:10.1038/nature04235

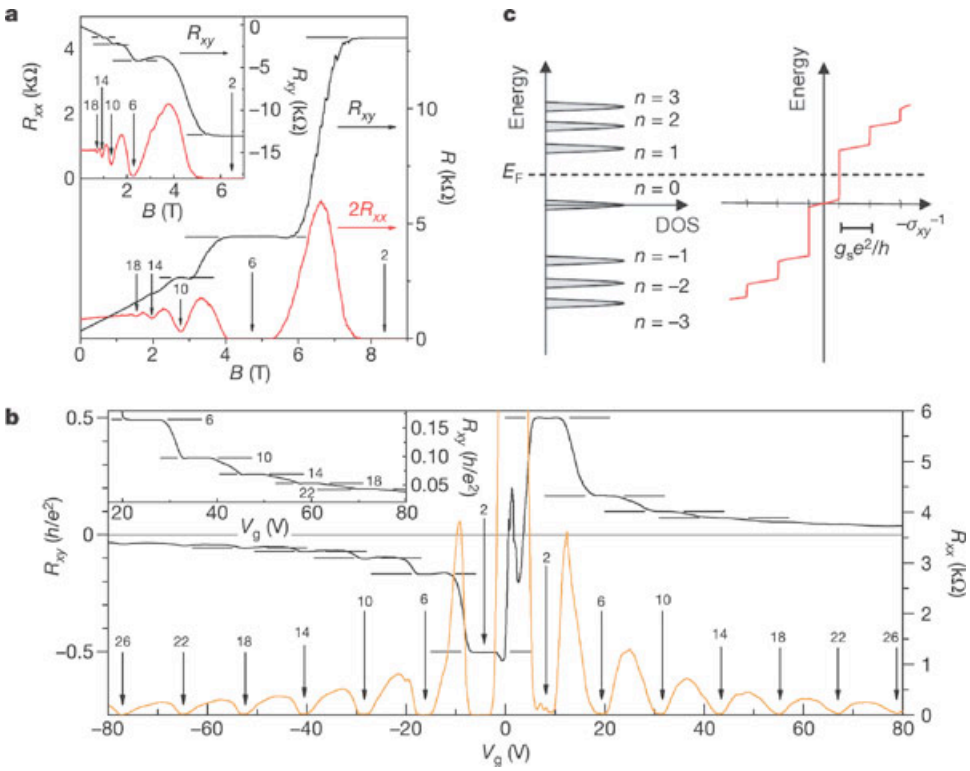

a, Hall resistance (black) and magnetoresistance (red) measured in the device in Fig. 1 at T = 30 mK and Vg = 15 V. The vertical arrows and the numbers on them indicate the values of B and the corresponding filling factor nu of the quantum Hall states. The horizontal lines correspond to h/e2nu values. The QHE in the electron gas is shown by at least two quantized plateaux in Rxy, with vanishing Rxx in the corresponding magnetic field regime. The inset shows the QHE for a hole gas at Vg = -4 V, measured at 1.6 K. The quantized plateau for filling factor nu = 2 is well defined, and the second and third plateaux with nu = 6 and nu = 10 are also resolved. b, Hall resistance (black) and magnetoresistance (orange) as a function of gate voltage at fixed magnetic field B = 9 T, measured at 1.6 K. The same convention as in a is used here. The upper inset shows a detailed view of high-filling-factor plateaux measured at 30 mK. c, A schematic diagram of the Landau level density of states (DOS) and corresponding quantum Hall conductance (sigmaxy) as a function of energy. Note that, in the quantum Hall states, Unfortunately we are unable to provide accessible alternative text for this. If you require assistance to access this image, or to obtain a text description, please contact npg@nature.com. The LL index n is shown next to the DOS peak. In our experiment the Fermi energy EF can be adjusted by the gate voltage, and Rxy-1 changes by an amount gse2/h as EF crosses a LL.